Available online at www.sciencedirect.com

ScienceDirect

Procedia Structural Integrity 81 (2026) 321–326

Structural Integrity Procedia

www.elsevier.com/locate/procedia

VIII International Conference "In-service Damage of Materials: Diagnostics and Prediction" (DMDP 2025)

Adhesion of Class A500C Steel Reinforcement to Concrete of Various Strengths

Oleksandr Chapiuk[a,*], Sergiy Filipchuk[b], Oleksandr Suvorov[a], Orest Pakholiuk[a], Dmytro Kusliuk[a], Iryna Zadorozhnikova[a], Olga Uzhegova[a], Anastasiia Shevchuk[a]

[a]*Lutsk National Technical University, Lvivska 75, 43018 Lutsk, Ukraine*
[b]*National University of Water and Environmental Engineering, Soborna 11, 33000 Rivne, Ukraine*

Abstract

New experimental data on the bond forces (bond stresses) between sickle-shaped ribbed steel reinforcement of class A500C and normal-weight concrete of various strength classes have been obtained. Pull-out tests of 16 mm diameter steel bars embedded in concrete prisms 5d (80 mm) high were conducted using a hydraulic tensile testing machine. An improved calculation methodology is proposed to ensure a reliable bond between A500C steel reinforcement and normal-weight concrete of varying strength levels. It was established that an increase in concrete strength leads to a proportional increase in the bond capacity of sickle-shaped reinforcement. A linear relationship between the maximum tangential bond stresses and concrete strength was identified, demonstrating good agreement with the experimental results.
The proposed linear dependence can be applied in the design of reinforced concrete structures for calculating the ultimate bond strength between sickle-shaped steel reinforcement and normal-weight concrete of various strength classes.

Keywords: bond between concrete and reinforcement, bond stress, strength, sickle-shaped profile, stress, reinforcement deformations.

1. Introduction

A wide range of materials is used in the construction of buildings and structures for various purposes (Dvorkin et al., (2021); Kos et al., (2022). These materials are very often applied in the assembly of load-bearing structures (Babych et al., (2019); Gomon et al., (2019); Kovalchuk et al., (2022); Bosak et al., (2021)), including concrete and reinforced concrete elements (Korniychuk et al., (2024); Filipchuk et al., (2024); Babych and Andriichuk, (2017); Drobyshynets et al., (2024); Parneta et al., (2024); Dovbenko et al., (2024)). The improvement of reinforced concrete structures depends on the development of a theory that adequately reflects the actual structural behaviour during service conditions (Konkol et al., (2019); Rybak et al., (2025); Sobczak-Piastka et al., (2020)). One of the key issues in this context is the determination of the bond between reinforcement and concrete, which plays a crucial role in ensuring the strength, stiffness, and crack resistance of reinforced concrete elements (Chapiuk et al., (2025); Babich et al., (2019); Filipchuk et al., (2023); Chapiuk et al., (2023)). Considerable progress has been made in studying the interaction between concrete and steel reinforcement, which is essential for both reinforced concrete theory and engineering practice.

* Corresponding author. Tel.: +38-099-227-19-87; fax: +0-000-000-0000 .
E-mail address: ochapiuk1983@gmail.com

2452-3216
10.1016/j.prostr.2026.03.056

However, a sufficiently substantiated and comprehensive theory of concrete-reinforcement bond has not yet been fully developed, especially considering the diversity of reinforcement types. Bond deterioration caused by external loading and other factors leads to changes in the structural behaviour of reinforced concrete elements. With increasing load levels and progressive bond degradation, continuous qualitative changes occur in the stress-strain state of the element.

Sickle-shaped ribbed reinforcement has been manufactured and used for more than two decades; however, existing studies on the bond behaviour of A500C reinforcement (DSTU 3760:2019; Eurocode 2:2004) with concretes of different strength classes remain insufficient for the accurate and efficient calculation of its anchorage length. This type of reinforcement is recommended for use in both non-prestressed and prestressed concrete structures.

Bond strength increases with an increase in the specified concrete strength class, a decrease in the water-cement ratio, and an increase in concrete age. In cases of insufficient anchorage at the ends of reinforcing bars, welded transverse bars or anchor plates are applied. When a reinforcing bar is pushed into concrete, the bond strength is higher than in pull-out tests, which is explained by the resistance of the surrounding concrete to the transverse expansion of the compressed bar.

The objective of this study is to analyze experimental data on the influence of concrete strength on the bond behaviour of A500C reinforcement and to establish the corresponding relationship under single short-term and repeated loading conditions.

Nomenclature

f_{cube}	cubic strength of concrete
f_{prism}	prismatic strength of concrete
σ_u	temporary tensile strength of rods
E_s	initial modulus of elasticity of reinforcement
A_s	area of rods
δ_u	slip (displacement) of the free end of the rod relative to the end of the prisms
σ_{s0m}	stress in the rod at δ_u=0.2 mm
$\sigma_{0,2}$	0.2% proof stress of reinforcement
σ_s	stress in the rod (beginning of slippage)
τ_{um}	tangential stresses

2. Methods of experimental research

The research task was addressed using concrete prisms with a square cross-section, having a side length of 150 mm and a height of 5d, where d = 16 mm is the bar diameter (i.e., 80 mm). The reinforcing bars were positioned in the concrete prisms so that their longitudinal axes coincided, while the protruding parts of the bars allowed fixing one end in the grips of the hydraulic tensile testing machine and measuring, at the other (free) end, the displacement relative to the end face of the concrete prism (Fig. 1a). The mechanical properties of 16 mm diameter A500C steel reinforcing bars were determined by uniaxial tensile tests performed on a hydraulic testing machine in accordance with the standard procedure (Table 1). The load was applied to the bar in increments of 1.0 kN. During loading, the displacement of the free end of the bar relative to the prism face was measured using a dial gauge indicator with a resolution of 0.001 mm, while the bar deformation relative to the concrete prism was measured using a Huggenberger mechanical extensometer with a 20 mm gauge length and a resolution of 0.001 mm (Fig. 1b).

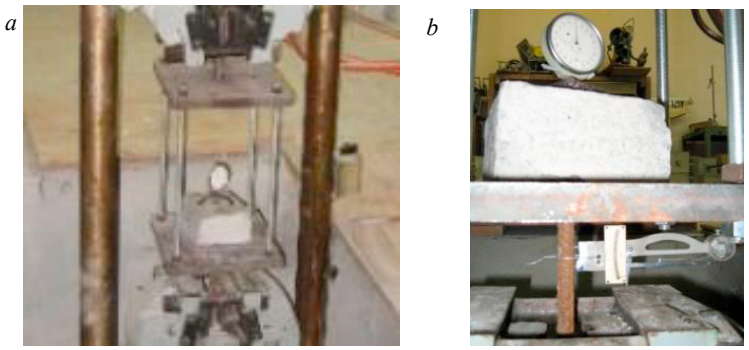

Fig. 1. General view of specimen testing in the hydraulic tensile machine (a) and measurement of reinforcement displacement using a dial gauge and bar deformation using a Huggenberger extensometer (b).

According to BS 4449:1997, the bond limit state between reinforcement and concrete is defined as the condition at which the slip of the free end of the reinforcing bar relative to the prism face reaches δ_u = 0.2 mm. Therefore, this value of δ_u corresponds to the reinforcement stress σ_{s0}.

Table 1. Mechanical properties of 16 mm diameter A500C steel reinforcing bars

Diameter, mm	Cross-sectional area, mm²	0.2% proof stress $\sigma_{0,2}$, MPa	Modulus of elasticity E_s, MPa	Ultimate tensile strength σ_u, MPa
16	201.5	498	200000	675

The mechanical properties of concretes of different strength classes were determined by testing 150 mm concrete cubes and 150 × 150 × 600 mm prisms, which were cast simultaneously with the main specimens (Table 2). The concrete properties are reported at the age corresponding to the start of testing of the main specimens (55–72 days).

Table 2. Mechanical properties of concrete

Concrete class	Cubic compressive strength f_{cube}, MPa	Prismatic compressive strength f_{prism}, MPa	Initial modulus of elasticity, E_b , MPa
C12/15	17.8	12.6	210000
C16/20	23.5	16.5	220000
C20/25	31.1	21.7	230000
C25/30	39.5	27.5	260000

3. Results and discussion

For each concrete strength class (C12/15, C16/20, C20/25, and C25/30), seven twin specimens were tested (Fig. 2). Three specimens from each group were subjected to single monotonic loading up to failure in order to determine the ultimate bond capacity between reinforcement and concrete. In addition, the bond behaviour of Ø16 mm sickle-shaped A500C reinforcement embedded in concretes of different strength classes was investigated under repeated loading. For this purpose, four specimens of each concrete class were subjected to 10 cycles of repeated loading up to 0.6 of the ultimate load, corresponding to service load conditions. During the 11th cycle, the specimens were intentionally loaded to failure. The experimental results indicated sufficient uniformity in concrete properties within each twin-specimen group.

Fig. 2. General view of the specimens.

Figure 3 presents the slip diagrams δ for specimens P-12/15k-1,2,3. In the specimen notation, the first numbers indicate the design concrete strength class, while the subsequent number denotes the specimen number. The letter “k” indicates specimens subjected to monotonic loading up to failure, whereas the letter “p” denotes specimens tested under repeated loading conditions. For specimens P-12/15k-1,2,3, the slip value $\delta_u = 0.2$ mm was reached at reinforcement stresses of $\sigma_{s0} = 74.5$, 72.3, and 69.5 MPa, respectively, with an average value of $\sigma_{s0m} = 72.1$ MPa. The standard deviation of stresses relative to the mean value was 2.5 MPa, corresponding to a coefficient of variation $\upsilon = 0.0346$. These statistical indicators confirm the high homogeneity of this group of specimens. For the remaining specimen groups, the coefficient of variation ranged within $\upsilon = 0.0295$-0.0843; therefore, further analysis was performed using average values for each group.

In all specimens, slip initiated at approximately the same stress level in the reinforcement; at $\sigma_s = 9.95$ MPa, the slip was $\delta = 0.001$ mm. Subsequently, the magnitude of bar slip was significantly influenced by concrete strength. Thus, at $\sigma_s = 69.5$ MPa, the slip values in specimens P-12/15k, P-16/20k, P-20/25k, and P-25/30k were $\delta = 0.126$, 0.034, 0.016, and 0.011 mm, respectively.

The bond limit state, corresponding to $\delta = \delta_u = 0.2$ mm, occurred at reinforcement stresses of $\sigma_s = \sigma_{s0} = 72.1$, 87.2, 132.6, and 160.1 MPa for specimens P-12/15k, P-16/20k, P-20/25k, and P-25/30k, respectively. It should be noted that specimens P-25/30k did not fail immediately after reaching $\delta_u = 0.2$ mm, but continued to resist reinforcement pull-out up to $\delta = 0.28$ mm, after which longitudinal splitting of the prisms along the reinforcing bars occurred. In this case, the reinforcement stress was $\sigma_s = 74.6$ MPa.

With increasing concrete strength, the difference between δ_u = 0.2 mm and the slip value immediately proceeding complete prism failure decreases, and for specimens P-25/30k, this difference was practically negligible (Fig. 4).

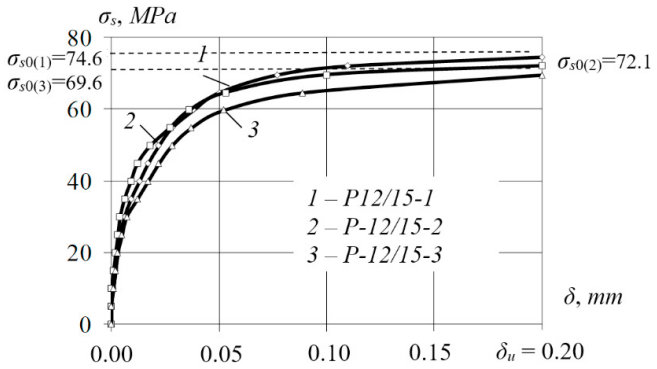

Fig. 3. Variation of bar slip δ during loading of specimens P-12/15k-1,2,3 (σ_s – reinforcement stress)

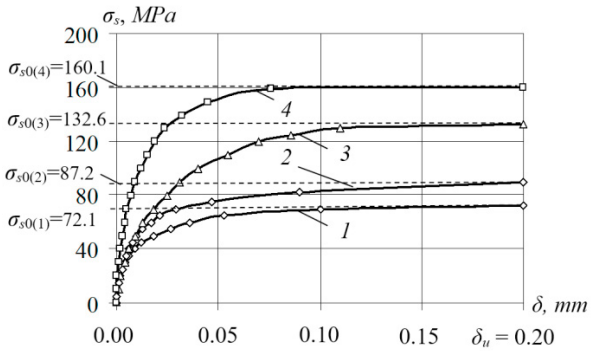

Fig. 4. Relationship between bar slip δ and reinforcement stress σ_s: 1 – specimens P-12/15k; 2 – P-16/20k; 3 – P-20/25k; 4 – P-25/30k.

During the first loading cycle of specimens P-12/15p, the average displacement of the reinforcement relative to concrete at the maximum repeated load level (σ_s = 39.8 MPa) was 0.011 mm, while the residual slip after unloading amounted to 0.003 mm. During the second loading and unloading cycle, the maximum slip was 0.012 mm. Residual deformations increased to 0.004 mm after unloading of the seventh cycle. After the eighth cycle, deformations stabilized at 0.014 mm (total) and 0.004 mm (residual). During the 11th cycle, a slip of 0.2 mm was reached at σ_{s0m} = 73.6 MPa, and specimen failure occurred at σ_s = 74.6 MPa (Fig. 5).

For specimens P-16/20p, the average displacement of the free end of the reinforcement relative to the prism face at the maximum repeated load level (σ_s = 52.2 MPa) during the first cycle was 0.015 mm, while the residual slip amounted to 0.003 mm. From the second to the seventh cycle, both total and residual slips increased by approximately 0.001 mm per cycle, reaching 0.023 mm and 0.008 mm, respectively, at the seventh cycle (Fig. 5). From this cycle onward, slip stabilization occurred. A slip of 0.2 mm was reached during the 11th cycle at σ_{s0m} = 89.5 MPa, while specimen failure occurred at σ_s = 91.2 MPa.

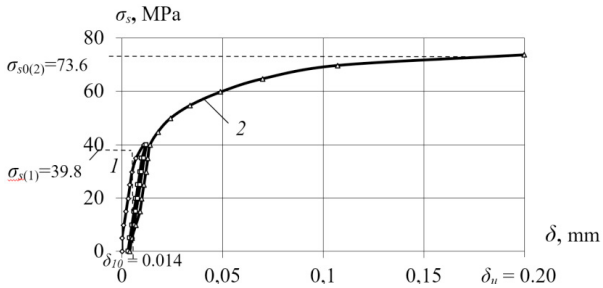

Fig. 5. Variation of bar slip δ versus reinforcement stress σ_s in specimen P-12/15p: 1 – first cycle; 2 – eleventh cycle (cycles 2-8 omitted).

Specimens P-20/25p were subjected to ten loading cycles up to a maximum stress of σ_s = 79.6 MPa. After the first cycle, the total displacement of reinforcement relative to concrete was 0.018 mm, with a residual slip of 0.006 mm (Fig. 6). During the second cycle, the maximum slip reached 0.020 mm, and the residual slip was 0.007 mm. Deformations increased slightly with each subsequent cycle, without full stabilization. After the tenth cycle, the total and residual slips were 0.031 mm and 0.013 mm, respectively. During the 11th cycle, a slip of 0.2 mm occurred at σ_{s0m} = 132.8 MPa, at which load the specimen failed.

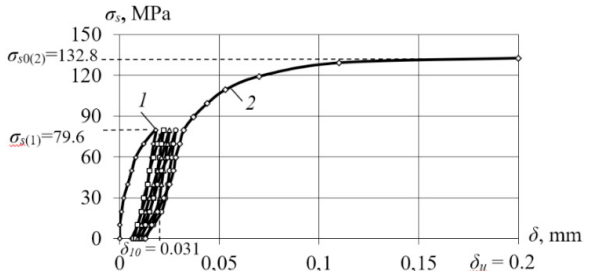

Fig. 6. Variation of bar slip δ versus reinforcement stress σ_s in specimen P-20/25p: 1 – first cycle; 2 – eleventh cycle (cycles 2–7 omitted)

For specimens P-25/30p, during the first cycle, the displacement of reinforcement relative to concrete at the maximum repeated stress level (σ_s = 94.5 MPa) was 0.011 mm, with a residual slip of 0.002 mm. During the second cycle, the maximum and residual slips were 0.012 mm and 0.003 mm, respectively. Stabilization of total and residual deformations occurred during the third cycle, reaching 0.013 mm and 0.003 mm, respectively. During the 11th cycle, a slip of 0.2 mm was reached at σ_{s0m} = 146.7 MPa.

After repeated loading up to 0.6 of the ultimate load, deformation stabilization occurred between the fourth and sixth cycles, while total slips did not exceed 0.03 mm, corresponding to approximately 15% of the ultimate slip value of 0.2 mm. The maximum stresses recorded during the 11th cycle were consistent with those obtained under single short-term loading.

Based on the experimental results, the average maximum tangential bond stresses τ_{um} were calculated for each group of specimens, assuming a uniform distribution along the embedded length of the bar, according to Eq. (1).

$$\tau_{um} = \sigma_{s0} A_s/(\pi d l_{an}). \quad (1)$$

Statistical analysis of the obtained results indicates that, for 16 mm diameter reinforcing bars, a linear relationship may be adopted between the maximum tangential bond stresses τ_{um} and the prismatic compressive strength of concrete f_{prism} (Fig. 7a), expressed by Eq. (2).

$$\tau_{um} = 0.3 \cdot fprism. \quad (2)$$

The coefficient of determination for this approximation is R^2 = 0.952, indicating good agreement with the experimental data.

A linear relationship was also observed between the reinforcement stresses σ_{s0} and the prismatic compressive strength of concrete f_{prism} (Fig. 7b), with a coefficient of determination R^2 = 0.975.

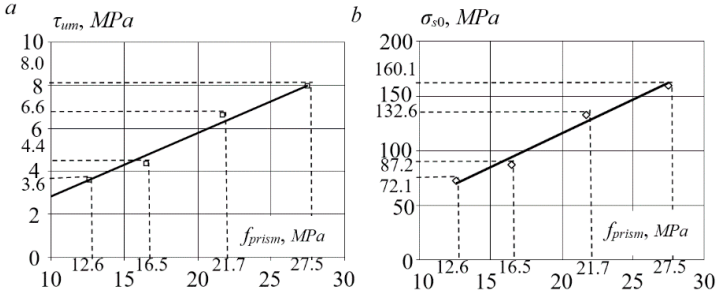

Fig. 7. Dependence of the average ultimate tangential bond stresses τ_{um} (a) and reinforcement stresses σ_{s0} (b) on concrete strength f_{prism}.

4. Conclusions

As a result of pull-out tests of 16 mm diameter steel reinforcing bars from concrete prisms using a hydraulic tensile testing machine, new experimental data on the bond behaviour of sickle-shaped A500C reinforcement depending on the strength of

normal-weight concrete were obtained. It was established that an increase in concrete strength is accompanied by a proportional increase in the bond capacity between sickle-shaped reinforcement and concrete. A linear relationship between the maximum tangential bond stresses and concrete strength was identified, demonstrating good agreement with the experimental results. The proposed linear relationship may be applied in the design of reinforced concrete structures to calculate the ultimate bond strength of sickle-shaped steel reinforcement embedded in normal-weight concretes of various strength classes.

References

Babich Y, Filipchuk, S, Karavan V., Sobczak-Piastka J., 2019. Research of basic mechanical and deformative properties of high-strength fast-hardening concretes. AIP Conference Proceedings 2077, 020003.

Babych, E.M., Andriichuk, O.V., 2017. Strength of Elements with Annular Cross Sections Made of Steel-fiber-Reinforced Concrete Under One-Time Loads. Mater Sci 52, 509–513.

Babych, Y.M., Savitskiy, V.V., Andriichuk, O.V., Ninichuk, M.V., Kysliuk, D.Y., 2019. Results of experimental research of deformability and crack-resistance of two span continuous reinforced concrete beams with combined reinforcement. IOP Conference Series: Materials Science and Engineering 708(1), 012043.

Bosak, A., Matushkin, D., Dubovyk, V., Homon, S., Kulakovskyi, L., 2021. Determination of the concepts of building a solar power forecasting model. Scientific Horizons 24(10), 9-16.

BRITISH STANDARD BS 4449: 1997. Specification for Carbon steel bars for the reinforcement of concrete.

Chapiuk, O., Kratiuk, O., Zadorozhnikova, I., Boiarska, I., Rud, V., Boiarskyi, M., Mudryy, I., Pelekh, A., 2025. Method for determining the minimum anchorage length of reinforcement in concrete: an experimental study. Procedia Structural Integrity 72, 308-314.

Chapiuk, O., Oreshkin, D., Hryshkova, A., Pakholiuk, O., Avramenko, Y., 2023. Adhesion of the Metal and Composite Fiberglass Rebar with the Heavyweight Concrete. Lecture Notes in Civil Engineering 299, 47-60.

Dovbenko, V., Kukhniuk, O., Homon, S., Ivaniuk, A., Aleksiievets, V., Savytska, O., Kulakovskyi, L., 2024. Study of the strength properties of concrete impregnated with a polymer composition. Procedia Structural Integrity 59, 702-709.

Drobyshynets, S., Babych, Y., Sunak, P., Zadorozhnikova, I., Parfentyeva, I., Pakharenko, V., Homon, S., 2024. Experimental and theoretical studies of fatigue of steel fibre reinforced concrete under low-cycle compression. Procedia Structural Integrity 59, 601-608.

DSTU 3760:2019, 2019. Prokat armaturnyy dlya zalizobetonnykh konstruktsiy. Zahal′ni tekhnichni umovy [Reinforcing bars for reinforced concrete structures. General technical conditions]. Ministry of Regional Development of Ukraine, Kyiv, pp. 18.

Dvorkin, L., Bordiuzhenko, O., Zhitkovsky, V., Gomon, S., Homon, S. (2021). Mechanical properties and design of concrete with hybrid steel basalt fiber. E3S Web of Conferences 264, article number 02030.

Eurocode 2, 2004: Design of Concrete Structures - Part 1-1: General rules and rules for buildings. CEN, Brussels, pp. 225.

Filipchuk, S., Karavan, V., Makarenko, R., Nalepa, O., Chapiuk, O., 2023. Study of reinforcement adhesion to concrete under static and dynamic loads. A*IP Conference Proceedings* 2949, 020007.

Filipchuk, S., Karavan, V., Nalepa, O., Chapiuk, O., Pakholiuk, O., 2024. Stability of slabs made of high-strength concrete subjected to dynamic influence. Procedia Structural Integrity 59, 588-594.

Gomon, S., Gomon, P., Pavluk, A., Podhorecki, A., 2019. Complete deflections of glued beams in the conditions of oblique bend for the effects of low cycle loads. AIP Conference Proceedings 2077, 020021.

Korniychuck, O., Masiuk, G., Homon, S., Aleksiievets, I., Chapiuk, O., Kaynts, D., Rizak, V., 2024. Deformability of reinforced concrete beams under the action of repeated alternating loads. Procedia Structural Integrity 59, 575-582.

Kos, Z., Klymenko, Y., Karpiuk, I., Grynyova, I., 2022. Bearing capacity near support areas of continuous reinforced concrete beams and high grillages. Applied Sciences (Switzerland) 12(2), 685.

Kovalchuk, V., Rybak, R., Parneta, B., Onyshchenko, A., Kvasnytsya, R., 2022. Determining patterns of the deformed state of the transport concrete pipe reinforced with a metal clamp under the action of static load. Eastern-European Journal of Enterprise Technologies 5 (7-119), 54–60.

Matviiuk, O., Homon, S., Petrenko, O., Vikhot, S., 2025. Operation of silor-modified wood in acidic environments: an experimental study. Lecture Notes in Civil Engineering 781, 237-244.

Parneta, B., Kovalchuk, V., Rybak, R., 2024. Methodology for Evaluating the Stress-Strain State of Strengthened Concrete Pipe Using the Finite Element Method with FEMAP with NX Nastran. Lecture Notes in Civil Engineering 604, 415-425.

Rybak, R., Kovalchuk, V., Parneta, B., 2025. Establishment of Regularities in the Stress-Strain State of Strengthened Reinforced Concrete Pipes Under Force Loads and Thermal Effects. Lecture Notes in Civil Engineering 781, 354–362.

Sobczak-Piastka J., Babich Y, Filipchuk, S, Karavan V., Nalepa, O., 2020. Research of deformative properties of concrete taking into account the descending branch of deformation. IOP Conference Series: Materials Science and Engineering 960(3), 032057.